Influence of Volume on Creep Behavior of Rock Salt Pillars

U.A.A. Mirza, E.L.J. Potts and A. Szeki

Department of Mining Engineering, University of Newcastle upon Tyne, England NE1 7RU

ABSTRACT

The prediction of long-term behavior of rock salt pillars can be based on laboratory experiments only if the effect of difference in volume of the laboratory specimen and of the underground pillar is firmly established. In order to establish the volume-effect for Cheshire rock salt, laboratory experiments were conducted in which the effect of a volume increase of 1,000 times was observed. The logarithmic relationship obtained by the experiments between creep rate and specimen size was extrapolated to actual pillar size.

INTRODUCTION

The influence of size or volume of test samples on the compressive, tensile and shear strength of rocks has been recognized for a long time (1). When the volume of prismatic or cylindrical sample is increasing then the specific rupture strength (i.e. σ/volume) of the sample is decreasing generally. In practice, this variation has to be taken into consideration when the design of pillar is based on the rock strength determined for small samples in the laboratory. The problem of assessing the strength of pillar is complicated further when the rock mass from which the pillars are formed exhibit time-dependent behavior, e.g. rock salt pillars. As far as the authors are aware, there is no information available regarding the "size—or volume effect" on the creep behavior of rock salt. Troxell et al (2) studied the effect of size and shrinkage on the creep of plain and reinforced concrete. Their study is irrelevant in respect of rock salt for obvious reasons, hence their findings are not referred to herewith. Due to lack of theoretical and empirical work on the volume-effect on creep a research scheme was initiated to investigate the variation in creep behavior of rock salt with increasing specimen size, with an aim in view to define an extrapolation procedure for underground large pillars.

DETERMINATION OF EXPERIMENTAL PARAMETERS

The dimension of test specimens and the applied load were selected on considerations based partly on mine parameters and partly on the availability and capacity of test equipment. Further restriction on test parameters were enforced by economic considerations. Theoretical considerations in respect of maximum stress levels prevailing in pillars within a production panel indicated that the maximum stress at the center of the panel is not exceeding the 17.5 MPa level. For this reason a slightly higher level, 21.0 MPa was chosen to be imposed on to the rock salt blocks to be tested in the laboratory. The largest block size was determined by the largest available creep rig.

Since the width to height ratio of the pillars in the panel were 2–2.5, then to maintain geometrical similarity between in situ pillars and laboratory specimens, a width to height ratio of 2 was chosen.

General features of the rock salt deposit. The salt beds in the Cheshire area occur within the Keuper Marl Series. The salt beds vary in thickness and quality and are separated by layers of marl. The salt and marl beds are identified by letters and are called Zones. At present, only the beds

Zone B and Zone F are mined. The crystal size in both zones is about 15mm.

Preparation and dimensions of test specimens. Altogether 34 specimens were cut from three blocks of 1 × 1 × 0.5m size. Two of the blocks came from Zone F and the third block from Zone B. All specimens were cut dry. Table 1 shows the number and dimensions of the specimens tested and the zone the block came from. It can be seen from the table that the ratio of volumes of the smallest and largest specimen is 1,000.

METHOD OF TESTING

In every single creep rig two specimens were loaded between smooth steel platens of a minimum thickness of 38mm. Whenever it was possible the two specimens belonged to the two different zones so that not only the volume effect could be revealed but also the differential behavior of the two salt bed zones under identical loading condition. The capacity range of the single loading rams varied from 50 tons through 100, 150, 200 to 1,000 tons. The largest blocks (0.221 m^3) were loaded by four 500 ton rams. The rams were individually calibrated to the required oil pressure. This calibration was necessary in order to avoid any discrepancy in the actual loading because the frictional losses varied from ram to ram. To avoid loss in load and to maintain a reasonable pressure control accumulators were coupled into every single hydraulic circuit and these were pressurized to the required levels by Nitrogen gas. Examples of testing arrangements are shown in Figures 1 and 2.

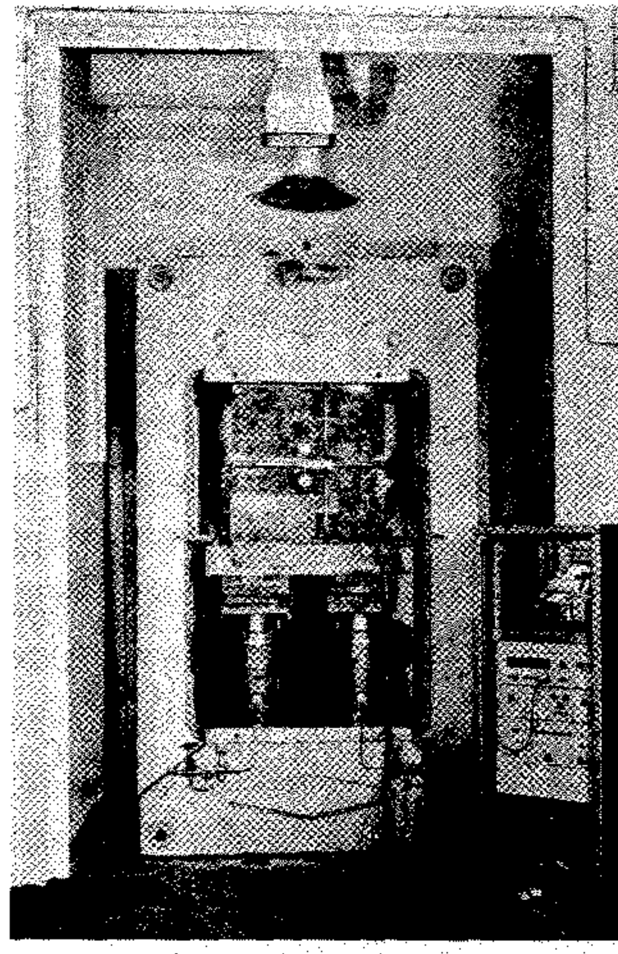

Figure 1. 2,000 ton creep rig.

TABLE 1

Specimen Dimensions and Number of Tests

Zone	Number	Dimensions m	Volume $\times 10^{-6}$ m^3	Log_{10} Vol
B F	5 7	0.0762 × 0.0762 × 0.0381	221.2	2.34479
B F	4 4	0.1270 × 0.1270 × 0.0635	1024.2	3.01038
B F	4 2	0.1905 × 0.1905 × 0.09525	3456.6	3.53865
F	2	0.254 × 0.254 × 0.127	8193.5	3.91347
F	2	0.3556 × 0.3556 × 0.1778	22483.1	4.35186
F	2	0.4572 × 0.4572 × 0.2286	47784.7	4.67929
B F	1 1	0.762 × 0.762 × 0.381	221225.4	5.34483
B Total	14			
F Total	20			
	34			

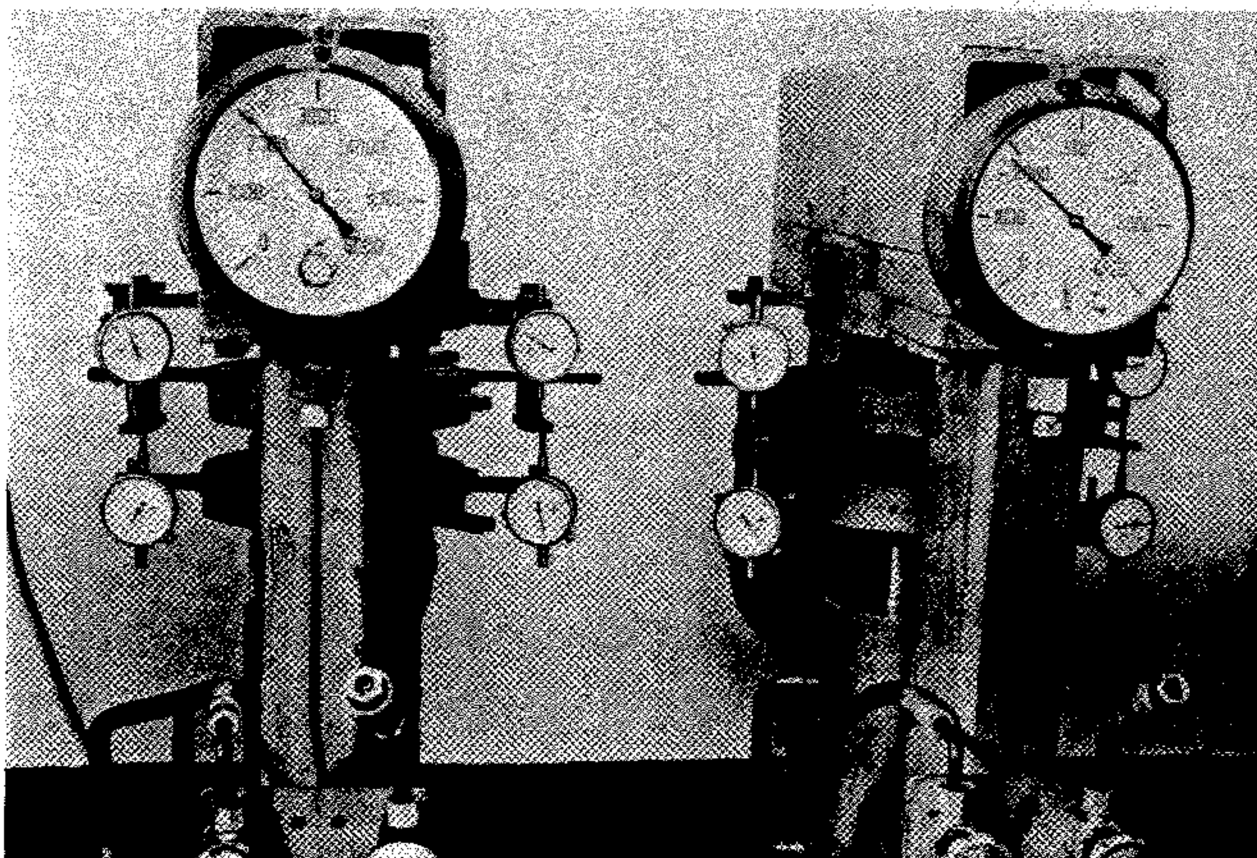

Figure 2. 50 ton creep rig.

With the 2,000 ton creep rig precautions have to be taken to prevent eccentric loading due to inequal rising of the pistons of the four rams.

Safety micro switches were installed at the four corners above the lower platen and were attached to the outside frame of the rig as shown in Fig. 3. Initially the switches were placed at a distance of 1cm above the lower platen and were connected into the control circuit of the hydraulic power pack. Had there been any eccentric loading, i.e. tilting of the lower platen due to the unequal rise of the four pistons, the switches would have generated a feedback signal activating a solenoid valve and switching off the hydraulic power pack.

The deformations of the blocks in the 2,000 ton creep rig were measured by four dial gauges. These were positioned at mid-width of the four sides of the specimens. At a later date two other dial gauges were mounted to measure the horizontal movement of the steel platen separating the two specimens. Four transducers were also used as another independent measurement of the deformation (see Fig. 3). The transducers were connected to a data logger which scanned the output from the transducers at certain time intervals. When the creep rate slowed down approximately three days after the start of the test, the transducers were removed from the rig and positioned at the next rig and a new test was started. All tests were carried out in air conditioned rooms with temperatures of 20°C and relative humidity of 60%.

In spite of precautions taken to maintain constant loading conditions at some of the hydraulic rigs a slight loss of pressure did occur, therefore the pressure had to be increased periodically. The stress, however, was not allowed at any time to decrease from its original value by more than 700 kPa. The accumulator of rig No. 12 did not function properly, resulting in loss of load and consequently required resetting of the oil pressure every few days. Ultimately, the test was stopped and the results of the deformations of two specimens from Zones B and F had to be discarded due to the step-like loading which distorted the results.

The hydraulic power pack which maintained constant load on the rig 18 functioned reasonably well. However, there were short periods where the pressure transducers were activated frequently, resulting in a slight increase in stress. This in effect subjected the specimens to a kind of

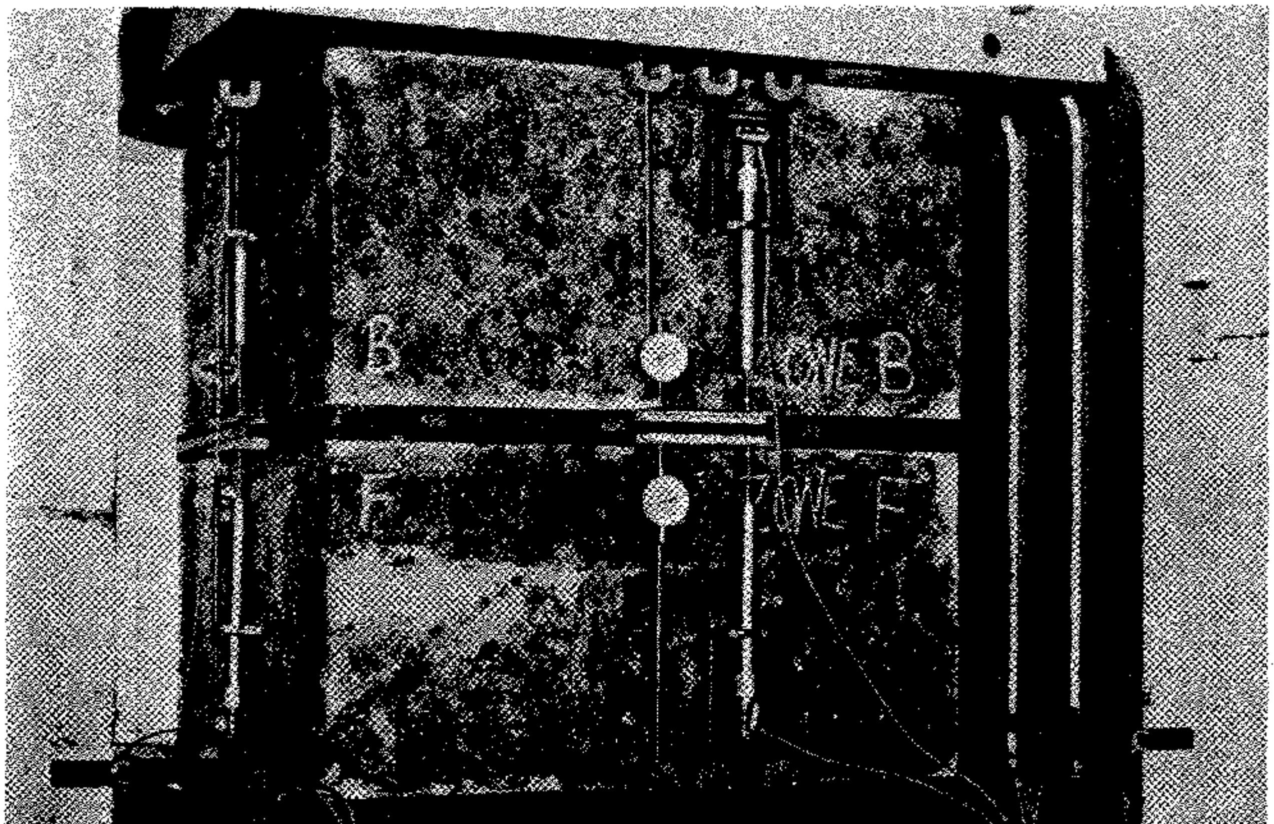

Figure 3. Close-up of measuring instruments.

cyclic loading. The specimens of volume 0.0478 m^3 seemed to have been squeezed at one side more than the other. Cracks across rock salt grains developed around 100 days after the test was initiated. It is suggested that these cracks were initially developed due to the fluctuating mode of stressing of the specimen. The fluctuating stresses would be picked up by the weakest zones in the specimen resulting in further opening and extension of cracks. This has to be borne in mind when the results of this particular test are analyzed.

METHOD OF ANALYSIS

The time-strain relationship of 32 tests are shown from Figure 4 to Figure 10 inclusive. Initially, the time-creep-strain relationship was approximated by a power function of the form of $\epsilon = At^m$, where A and m are constants, ϵ is the creep strain and t is time in days. The values of A and m for the 32 curves were formed by the linear regression method. For assessing the efficiency of the regression equation, different statistical indices were evaluated. The coefficient of correlation, (R), represents the degree of correlation between two sets of measurements. Another index is "the coefficient of alienation", k. It represents the lack of correlation between the two sets of measurements. The two indices R and k are represented by a circle of radius 1.0, i.e.

$$k^2 + R^2 = 1.0$$

$$\text{and} \quad k = (1 - R^2)^{0.5}$$

Therefore when R is 1.0 then 'k' is zero and it is implying perfect correlation. When R = 0.99, k = 0.14. However, when R = 0.5, then k = 0.866, i.e. the degree of relationship is less than that of the lack of relationship. It is only when R = 0.7071, then the two indices become equal.

From k or R another useful parameter can be derived, this parameter is the index of forecasting efficiency, I.F.E. (3) and is given by:

$$\text{I.F.E.} = 100\,(1 - k) = 100\,(1 - (1 - R^2)^{0.5})$$

The residuals from the regression equation are assumed to be normally distributed with zero mean. They are uncorrelated and independent of each other (4). To assess the degree of deviation from this pattern, Durbin and Watson (5) have suggested the test:

$$\text{D.W.} = \frac{\sum_{i=2}^{n} (r_i - r_{i-1})^2}{\sum_{i=1}^{n} r_i^2}$$

where r are the residuals

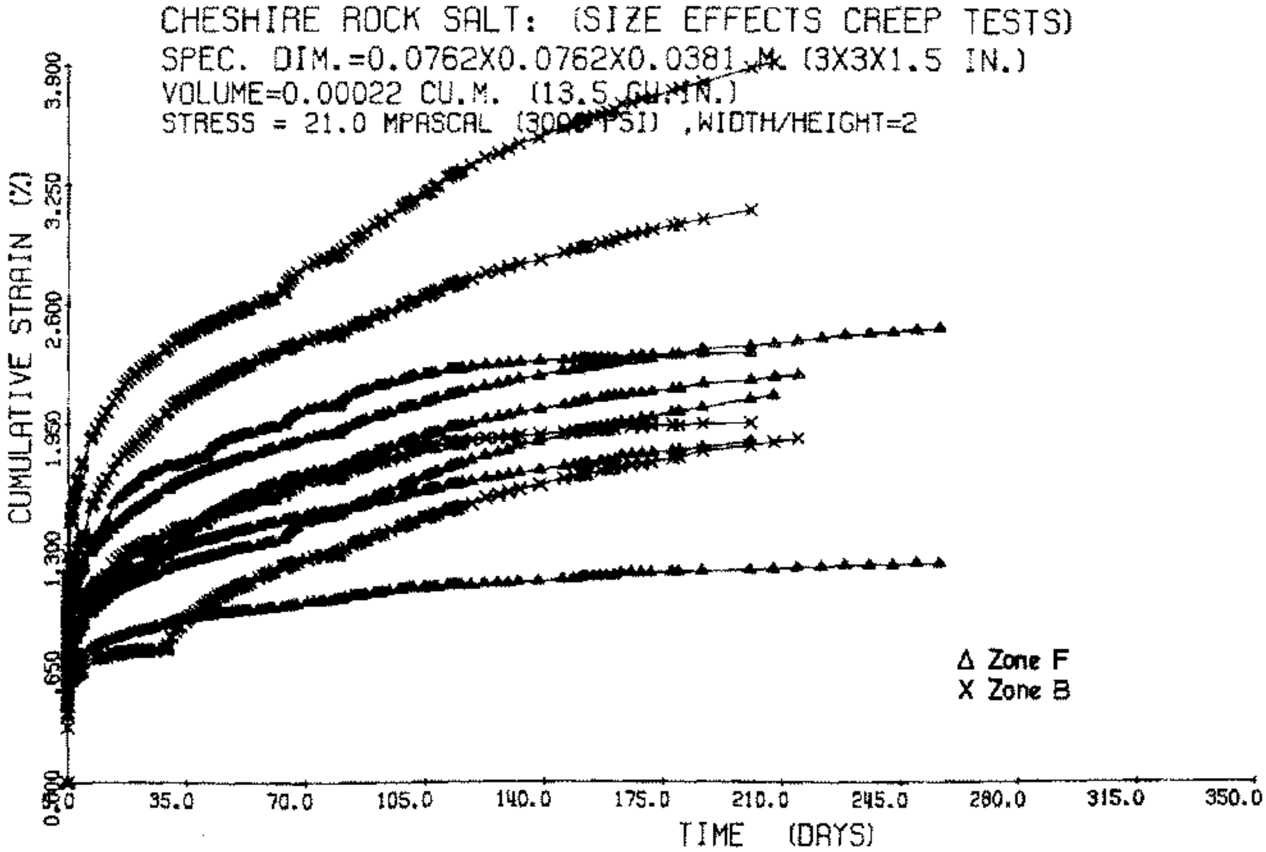

Figure 4. Creep curves.

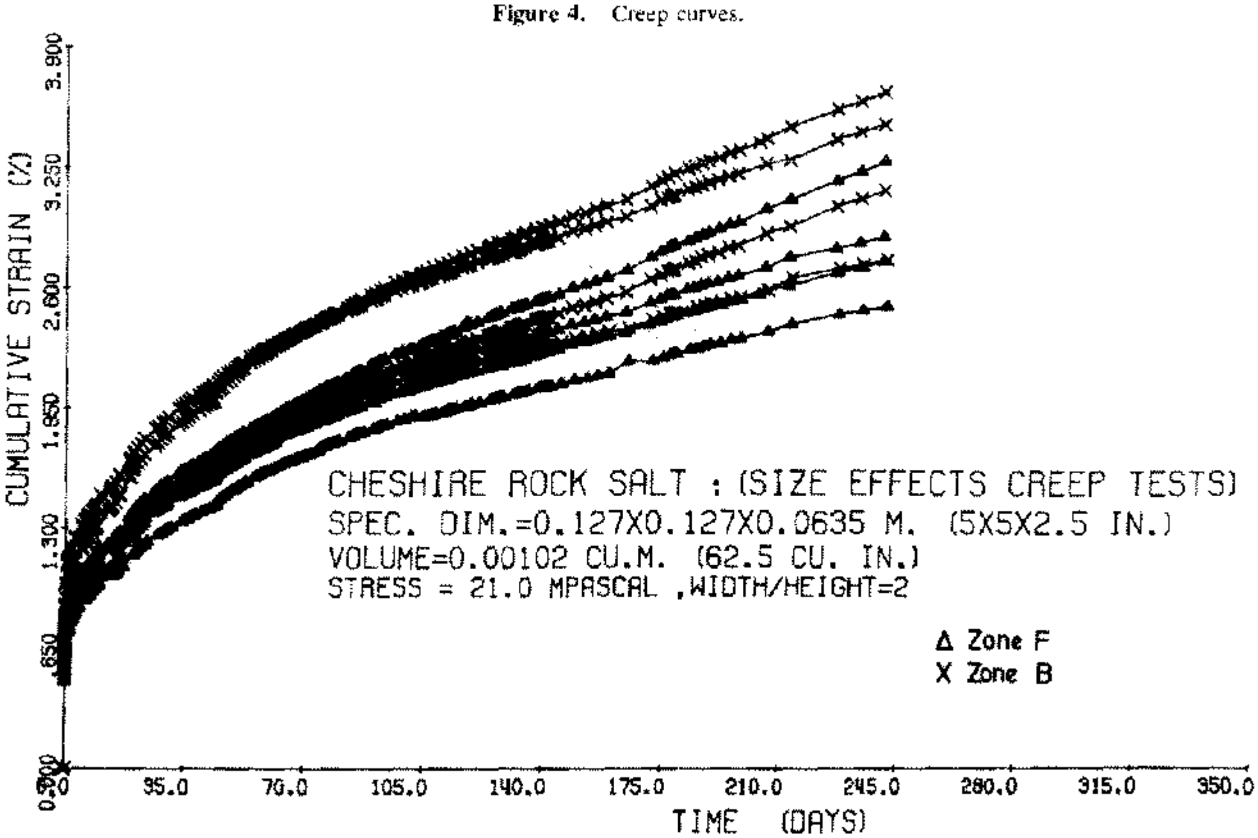

Figure 5. Creep curves.

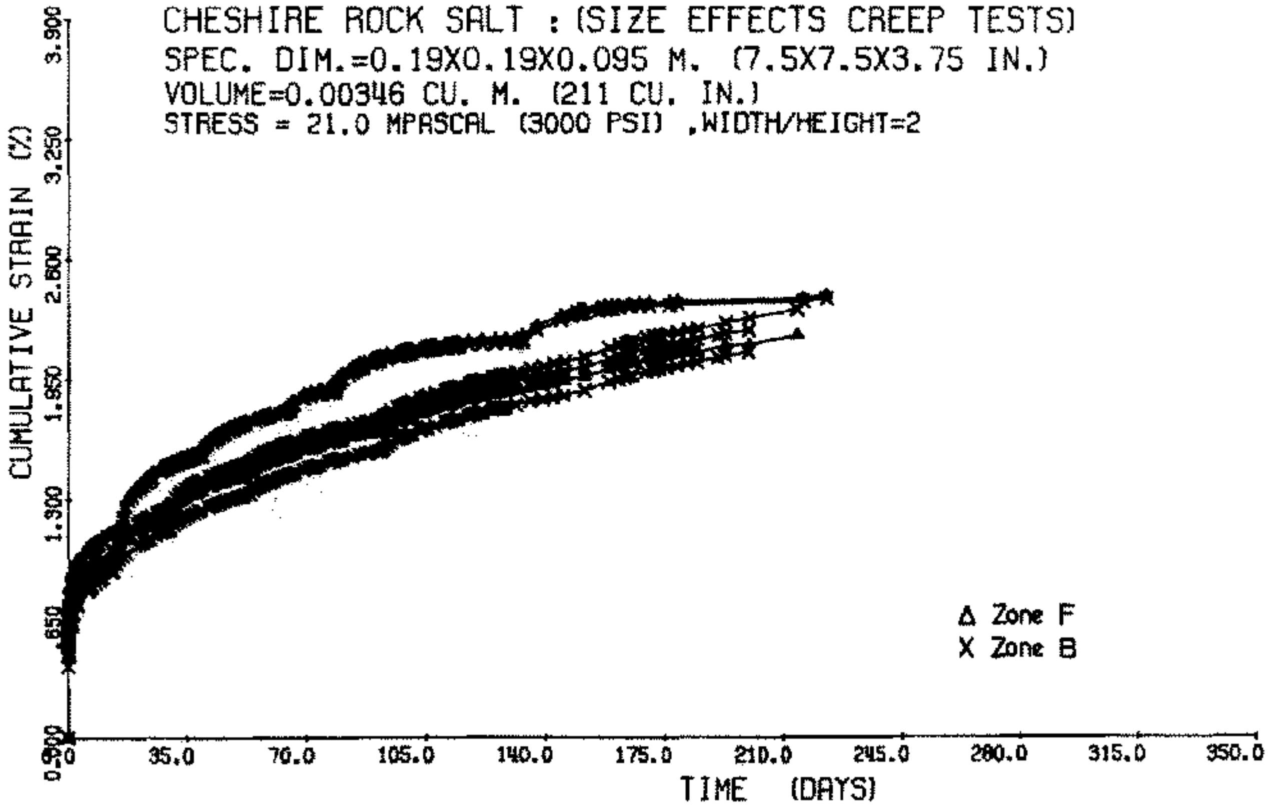

Figure 6. Creep curves.

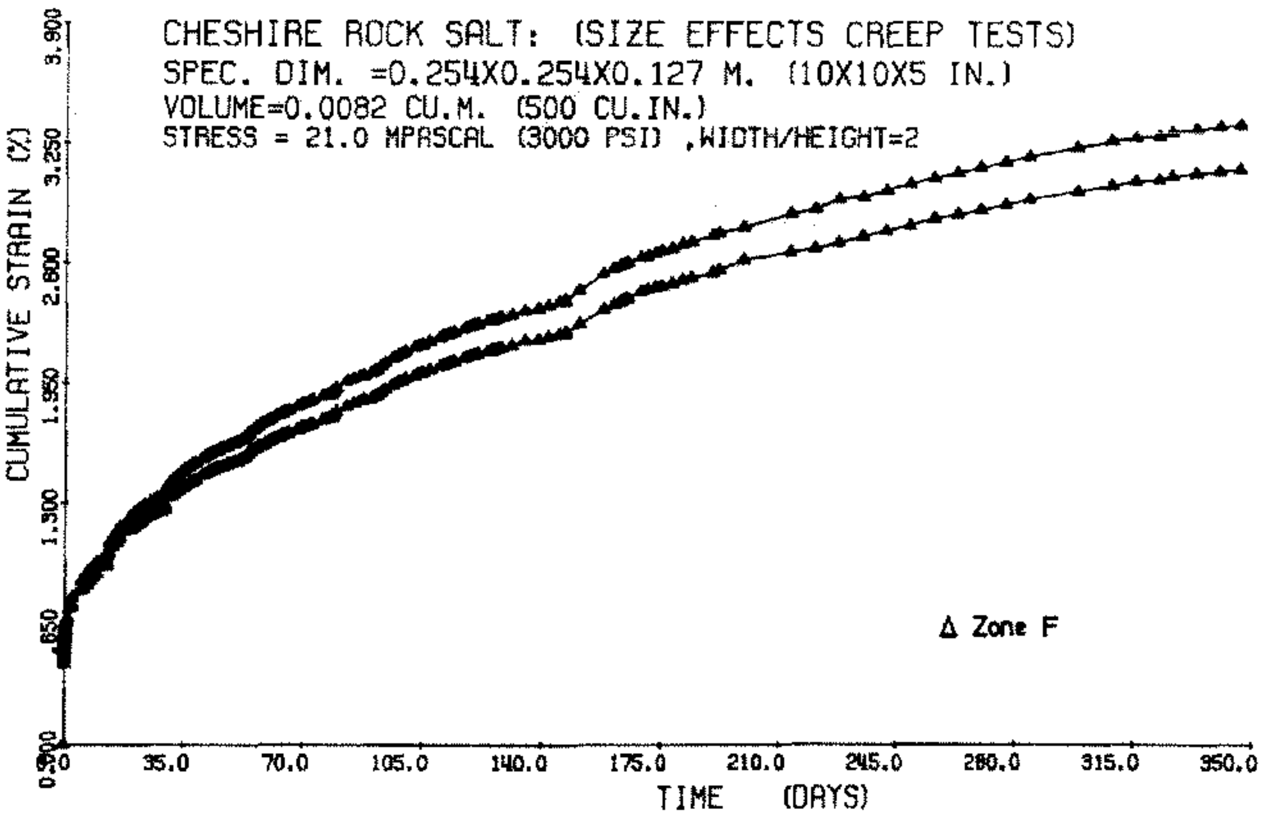

Figure 7. Creep curves.

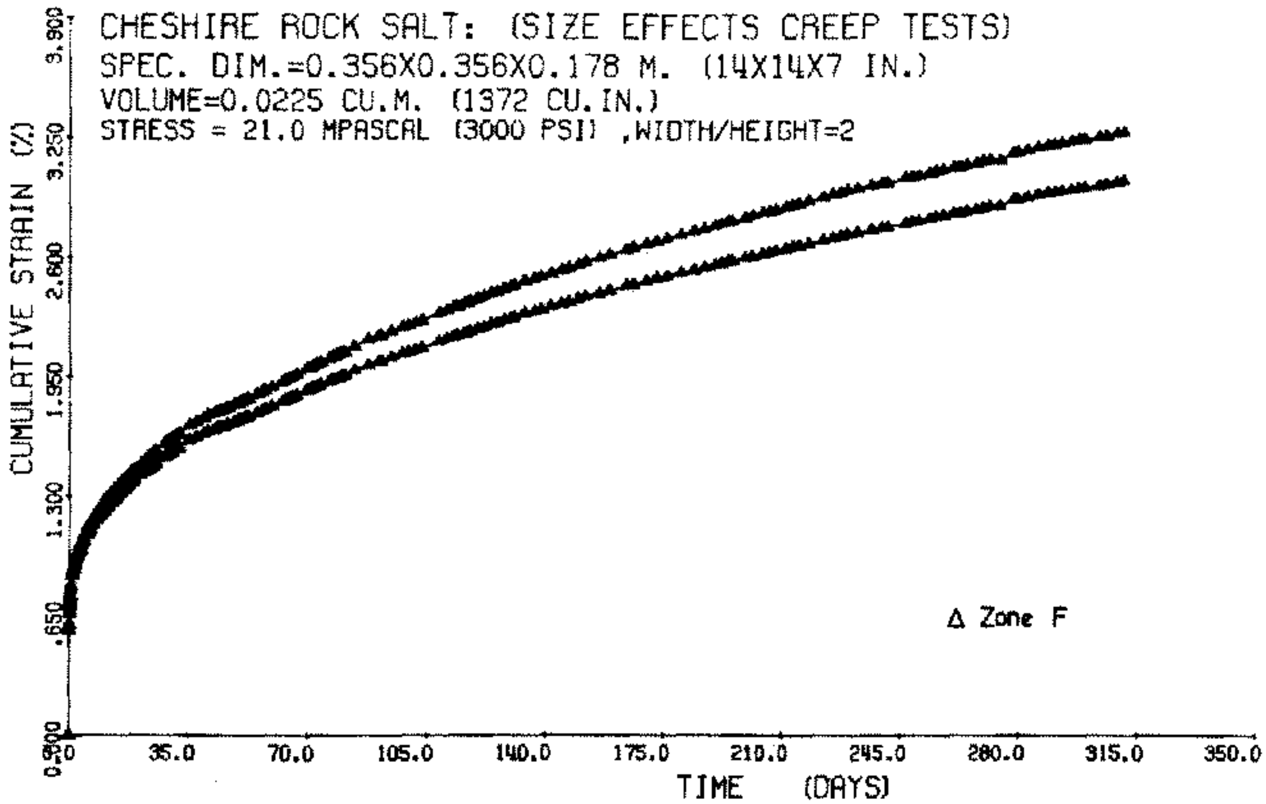

Figure 8. Creep curves.

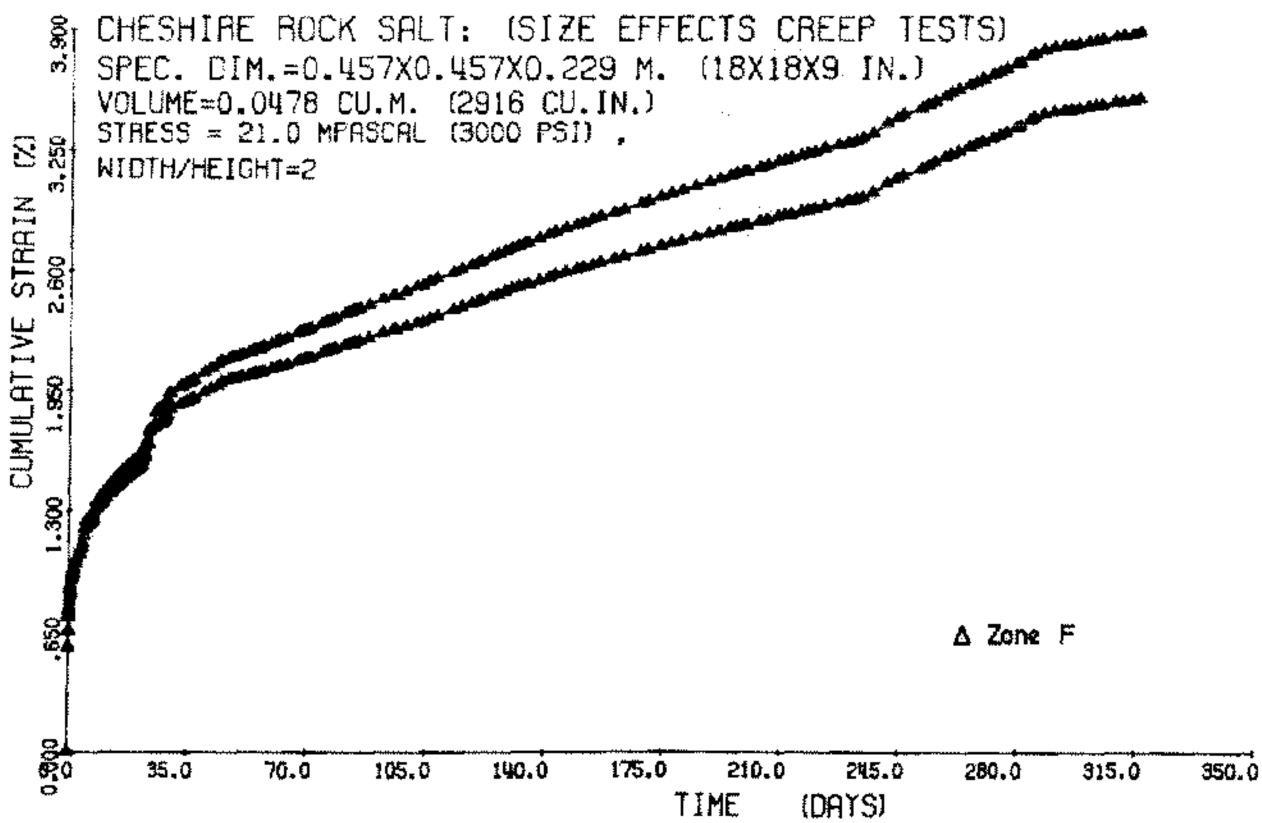

Figure 9. Creep curves.

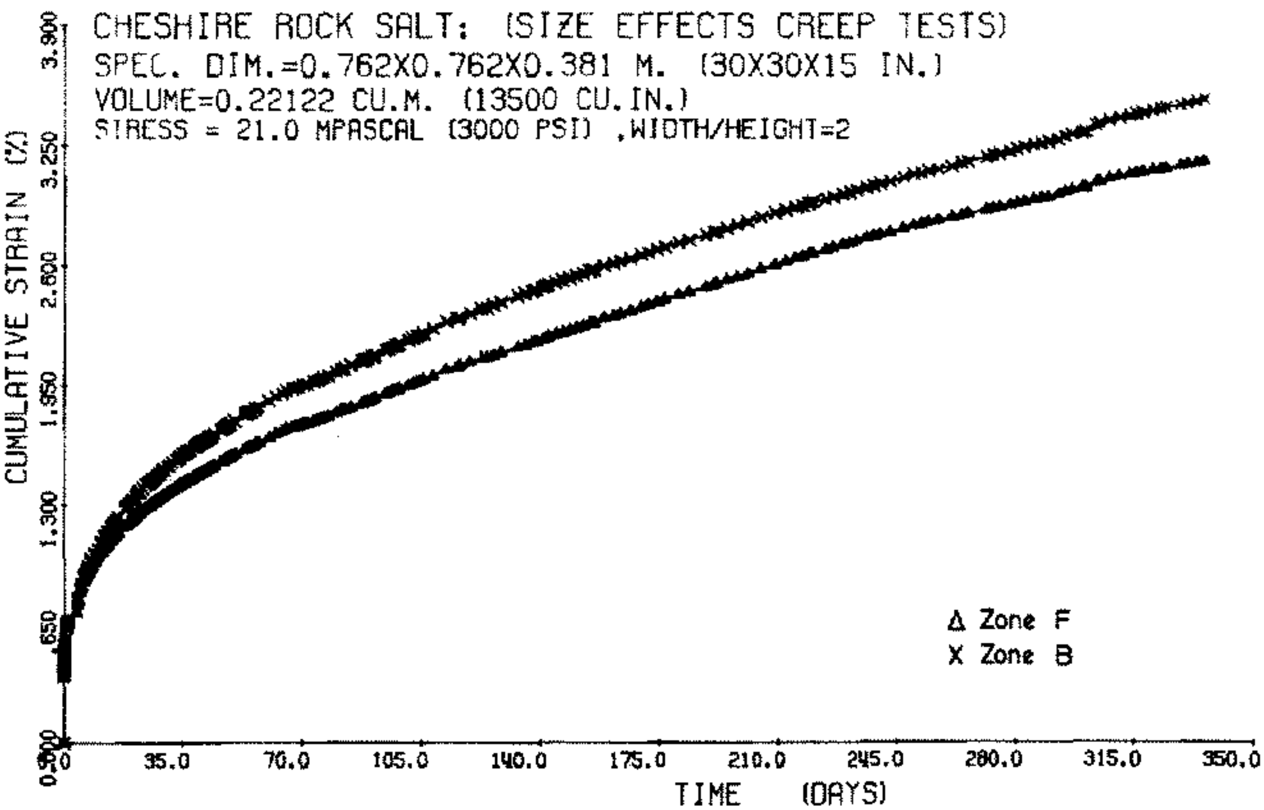

Figure 10. Creep curves.

Durbin and Watson have tabulated lower and upper limits for their statistics. If the calculated value is smaller than the lower limit, the hypothesis of non-correlation between the residuals is rejected in favor of positive serial correlation. If the calculated value is larger than the upper limit, the residuals are random. If the statistical value lies between the lower and the upper limits, then the test is inconclusive. Also, if D.W. is greater than 2 then a special procedure, similar to the one described above, applies.

During the testing of the specimens, it was usual to find that the original pressure reduced after a few minutes from the start of the test because the pressurized oil and nitrogen gas started to cool down. Therefore it was necessary to reset the pressure to the required level. In time, the heat inside the accumulator would be the same as the environment and then the reduction of pressure would be solely due to the hydraulic leakage. For the large specimens i.e. of volume 22.5×10^{-3} m^3, 47.8×10^{-3} m^3, and 221.2×10^{-3} m^3 the load applied hydraulically was controlled by the power pack through a pressure transducer. Each rig had its own power pack and there was no need for accumulators to be coupled into the hydraulic circuit, consequently there was no need for resetting of pressure. Therefore to make the results of the small and the large specimens comparable, it was decided to analyze the data from Day 5 onwards.

Using the time function described earlier, the parameters of the equations for the thirty-two tests are given in Table 2. The statistical indices are also included in the table.

In Table 2, the specimen number is designated so that the first number or letter refer to the rig number, the second letter denotes the position of the specimen in the testing rig. The abbreviations used in the table for the statistical parameters are:

R = Coefficient of correlation
k = Coefficient of alienation
I.F.E. = Index of forecasting efficiency
D.W. = Durbin and Watson statistics
Σr^2 = Sum of squares of the residuals

From Table 2 it is found that the parameters A and m do not show a significant variation with specimen size. However, the table indicates that when the specimens belong to the same zone, their behavior is alike when tested in a single rig. The overall picture is that m increases as the volume of the specimen becomes larger, implying a faster creep rate for larger specimens. This becomes apparent when the specimens of Zone F of volume 0.221×10^{-3}m^3 are compared with the large specimens, say, of volume 0.221 m^3. In all cases the coefficient of correlation, (R), is quite high

TABLE 2

Analysis of Data According to the Equation: $\epsilon = At^m$

Specimen No.	Volume 10^{-6} m^3	$A \times 10^{-3}$	m	R	k	IFE	D.W.	$\Sigma r_i^2 \times 10^{-5}$	Zone
				5–200 Days					
6.U.	221.2	9.976	0.214	0.99	0.13	87	0.054	0.963	B
8.L.	221.2	6.927	0.202	0.98	0.17	82	0.058	0.756	B
13.U.	221.2	2.567	0.366	0.97	0.25	74	0.204	3.557	B
15.U.	221.2	11.370	0.220	0.97	0.25	74	0.033	14.817	B
L.U.	1024.2	6.014	0.269	0.99	0.14	86	0.105	1.346	B
F.U.	1024.2	6.676	0.299	0.99	0.12	87	0.113	2.368	B
C.U.	1024.2	8.002	0.257	0.99	0.13	86	0.119	1.886	B
A.U.	1024.2	7.021	0.232	0.97	0.25	74	0.115	1.423	B
I.U.	3456.6	5.221	0.265	0.98	0.16	84	0.052	2.153	B
I.L.	3456.6	4.420	0.286	0.98	0.16	84	0.056	1.756	B
H.L.	3456.6	5.092	0.277	0.99	0.15	85	0.101	1.671	B
K.L.	3456.6	5.826	0.273	0.99	0.15	85	0.190	1.599	B
30.U.	221225.4	5.129	0.317	0.99	0.10	90	0.012	1.031	B
6.L.	221.2	6.595	0.189	0.98	0.16	84	0.049	0.436	F
8.U.	221.2	9.255	0.183	0.98	0.18	82	0.064	1.342	F
11.U.	221.2	5.459	0.140	0.97	0.25	75	0.176	0.155	F
11.L.	221.2	8.452	0.191	0.98	0.17	83	0.080	1.075	F
13.L.	221.2	6.158	0.237	0.98	0.20	80	0.161	2.329	F
15.L.	221.2	5.175	0.247	0.96	0.28	72	0.030	7.586	F
A.L.	1024.2	4.746	0.339	0.99	0.12	88	0.125	2.460	F
C.L.	1024.2	6.350	0.266	0.99	0.13	87	0.144	1.053	F
F.L.	1024.2	5.365	0.290	0.99	0.13	87	0.160	1.019	F
L.L.	1024.2	5.153	0.280	0.99	0.14	85	0.123	1.633	F
H.U.	3456.6	4.989	0.272	0.99	0.14	85	0.150	0.623	F
K.U.	3456.6	6.011	0.268	0.98	0.17	84	0.174	1.906	F
J.U.	8193.5	4.583	0.332	0.99	0.14	84	0.063	3.676	F
J.L.	8193.5	4.403	0.325	0.99	0.14	84	0.060	3.116	F
14.U.	22483.1	6.814	0.260	0.99	0.14	84	0.025	4.244	F
14.L.	22483.1	6.779	0.247	0.99	0.14	84	0.026	3.235	F
18.U.	47784.7	7.777	0.242	0.99	0.14	85	0.049	2.855	F
18.L.	47784.7	7.634	0.262	0.99	0.14	85	0.053	3.329	F
30.L.	221225.4	5.107	0.293	0.99	0.13	87	0.008	3.062	F
				5–300 Days					
J.U.	8193.5	4.447	0.340	0.99	0.14	86	0.049	5.532	F
J.L.	8193.5	4.269	0.334	0.99	0.13	86	0.044	4.875	F
14.U.	22483.1	6.490	0.275	0.98	0.14	85	0.020	8.318	F
14.L.	22483.1	6.477	0.260	0.99	0.14	85	0.021	6.600	F
18.U.	47784.7	7.164	0.282	0.98	0.15	84	0.015	19.771	F
18.L.	47784.7	7.292	0.261	0.98	0.16	83	0.014	17.788	F
30.U.	221225.4	4.815	0.311	0.99	0.13	86	0.003	11.494	B
30.L.	221225.4	4.970	0.327	0.99	0.10	90	0.005	4.057	F

and so is the index of forecasting efficiency. The residuals, however, seem to exhibit positive serial correlation when tested with tables given by Durbin and Watson since they are smaller than the tabulated lower limit for a given significance level. The number of observations, however, in all cases exceeds 100, which is the maximum number of observations for which the tables are compiled by Durbin and Watson. Because the number of observations was well over 100 the residuals seem to be correlated according to the suggestions of Draper and Smith (6). It was also found that as the duration of the test increased, the predicted strains became under estimated. This can be confirmed from the tests when the data were analyzed between 5 and 300 days, (see Table 2). The sum of squares of residuals gets larger and a major percentage of the error lies towards the end of the predicted curve, presumably because the number of readings taken is always greater at the early stages of the test and, as a result the regression curve is biased to satisfy the early readings.

It was decided, therefore, to follow another statistical evaluation and the data were analyzed for the period from 100 to 200 days. The equation chosen was the equation of a straight line, i.e.

$$\epsilon = A + Bt$$

Thus the creep rate, instead of being evaluated from the power law as $\dot{\epsilon} = Amt^{m-1}$, was taken as an average over the period from 100 to 200 days and was represented by the slope of the straight line, i.e. by B. The curves shown in Figures 4 to 10 do not invalidate the assumption of almost a secondary stage of creep. The constants of the equation and the statistical parameters are given in Table 3. Confidence intervals can be established by using the relationship given by Smillie (7), as:

$$\text{Confidence interval (C.I)} = \pm (C \cdot \text{'t'}_{(n-2)}),$$

$$\text{Where } C = \frac{\frac{1}{n-2}\Sigma(\epsilon_i - \epsilon_i')^2}{\Sigma t_i^2 - \frac{(\Sigma t_i)^2}{n}},$$

ϵ_i = actual strain, ϵ_i' = predicted strain

t_i = actual time

't' is Student's t − distribution for (n − 2) degrees of freedom, and n is the number of observations.

Thus from Table 3 the average creep rate for specimen 6.U is 50.51 $\mu\epsilon$/day. Within 95% confidence interval the range will be 48.83 $\mu\epsilon$/day-52.19 $\mu\epsilon$/day.

Table 3 shows a definite improvement prediction wise and also in the overall statistical picture. The sum of squares is minimal in most cases. The coefficient of alienation is reduced leading to a better forecasting efficiency of the equation. The Durbin-Watson statistic has also improved and in the case of specimen L.L., the hypothesis of serial correlation is rejected at 95% significance level. The table also indicates that there is an apparent volume effect in the creep rate. There is also a gradual increase in the creep rates for the largest specimens as the volume is increasing from 0.221×10^{-3} m^3 to 221.2×10^{-3} m^3. It can be seen from Figures 11 and 12 that there is a scatter in the creep rates for

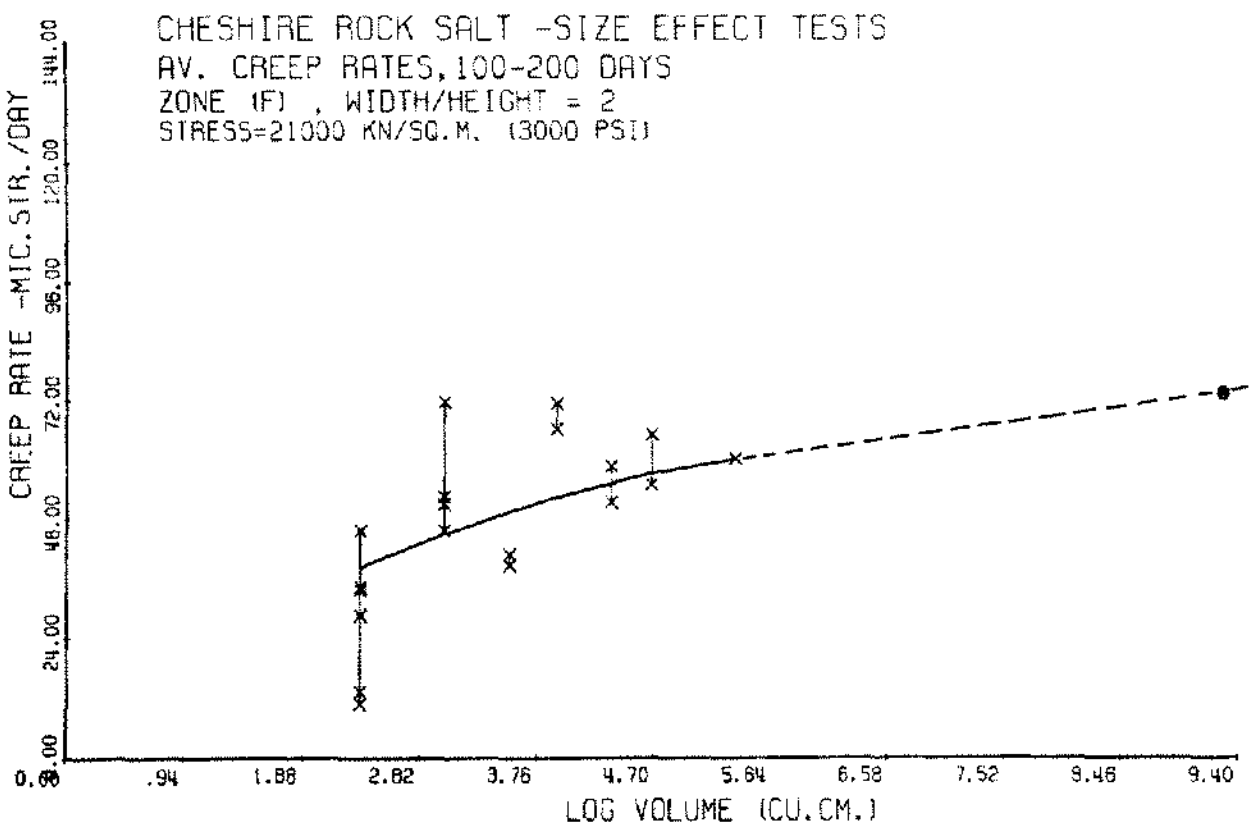

Figure 11. Creep rates for the period from 100 to 200 days as a function of log Volume for Zone F.

TABLE 3

Average Creep Rates for the Periods From:

Specimen No.	Volume	$A \times 10^{-2}$	B $\mu\epsilon$/day	C	R	k	IFE	D.W.	$\Sigma r_i^2 \times 10^{-3}$	No. Observations	Zone
					100–200 Days						
6.U.	221.2	2.134	50.51	0.822	0.99	0.09	91	0.294	5.733	34	B
8.L.	221.2	1.664	15.62	0.314	0.97	0.22	78	0.290	3.146	33	B
13.U.	221.2	1.000	43.40	0.973	0.99	0.13	87	0.286	8.027	34	B
15.U	221.2	2.454	74.48	1.533	0.99	0.12	88	0.251	2.076	35	B
L.U.	1024.2	1.649	45.53	0.241	0.99	0.04	96	0.481	1.196	49	B
F.U.	1024.2	1.935	71.95	0.400	0.99	0.03	96	0.381	2.578	41	B
C.U.	1024.2	1.976	63.34	0.326	0.99	0.05	95	0.395	1.940	48	B
A.U.	1024.2	1.525	66.06	0.470	0.99	0.05	95	0.187	4.297	49	B
H.L.	3456.6	1.384	46.05	0.415	0.99	0.05	94	0.375	2.087	40	B
I.U.	3456.6	1.371	43.37	0.241	0.99	0.06	94	0.413	2.411	41	B
I.L.	3456.6	1.228	44.34	0.360	0.99	0.05	94	0.483	1.736	41	B
K.L.	3456.6	1.679	39.85	1.791	0.97	0.21	75	0.209	18.641	33	B
30.U.	221225.4	1.578	63.68	0.555	0.99	0.06	94	0.221	4.775	44	B
6.L.	221.2	1.295	28.55	0.454	0.99	0.09	91	0.417	1.752	34	F
8.U.	221.2	2.093	13.24	0.722	0.95	0.29	71	0.232	4.087	33	F
11.U.	221.2	0.949	10.74	0.281	0.98	0.16	84	0.502	0.698	35	F
11.L.	221.2	1.721	34.32	0.801	0.99	0.13	87	0.387	5.672	35	F
13.L.	221.2	1.548	33.69	0.870	0.99	0.14	85	0.282	6.416	34	F
15.L.	221.2	1.203	45.78	0.908	0.99	0.11	88	0.261	7.274	35	F
L.L.	1024.2	1.422	45.79	0.267	0.99	0.03	96	1.866	1.564	50	F
F.L.	1024.2	1.533	51.07	0.185	0.99	0.02	98	1.136	0.553	41	F
C.L.	1024.2	1.628	52.63	0.297	0.99	0.04	95	0.368	1.816	49	F
A.L.	1024.2	1.547	71.86	0.445	0.99	0.05	95	0.502	4.326	50	F
H.U.	3456.6	1.353	40.89	0.469	0.99	0.06	93	0.396	2.659	70	F
K.U.	3456.6	1.719	38.67	1.793	0.97	0.25	75	0.194	18.682	33	F
J.U.	8193.5	1.402	71.58	1.307	0.98	0.11	88	0.150	22.902	43	F
J.L.	8193.5	1.303	66.31	1.221	0.98	0.11	88	0.132	19.979	43	F
14.U.	22483.1	1.676	58.81	0.554	0.99	0.05	94	0.214	4.220	40	F
14.L.	22483.1	1.597	51.62	0.491	0.99	0.05	94	0.213	3.317	40	F
18.U.	47784.7	1.875	65.26	0.617	0.99	0.06	93	0.155	4.525	38	F
18.L.	47784.7	1.784	55.10	0.613	0.99	0.07	93	0.156	4.456	38	F
30.F.	221225.4	1.355	60.13	0.219	0.99	0.02	98	0.489	0.742	44	F
					200–300 Days						
J.U.	8193.5	1.944	47.06	0.892	0.99	0.07	93	1.320	1.283	14	F
J.L.	8193.5	1.815	40.34	0.733	0.99	0.07	93	0.708	0.866	14	F
14.U.	22483.1	1.981	42.84	0.278	0.99	0.05	94	0.804	0.971	39	F
14.L.	22483.1	1.842	38.76	0.259	0.99	0.05	95	0.748	0.839	39	F
18.U.	47784.7	1.564	77.95	1.120	0.99	0.09	90	0.134	18.225	41	F
18.L.	47784.7	1.388	71.72	1.145	0.99	0.10	89	0.188	19.060	41	F
30.U.	221225.4	1.859	49.47	0.232	0.99	0.05	95	0.894	0.708	39	B
30.L.	221225.4	1.649	46.56	0.455	0.99	0.06	93	0.309	2.582	39	F

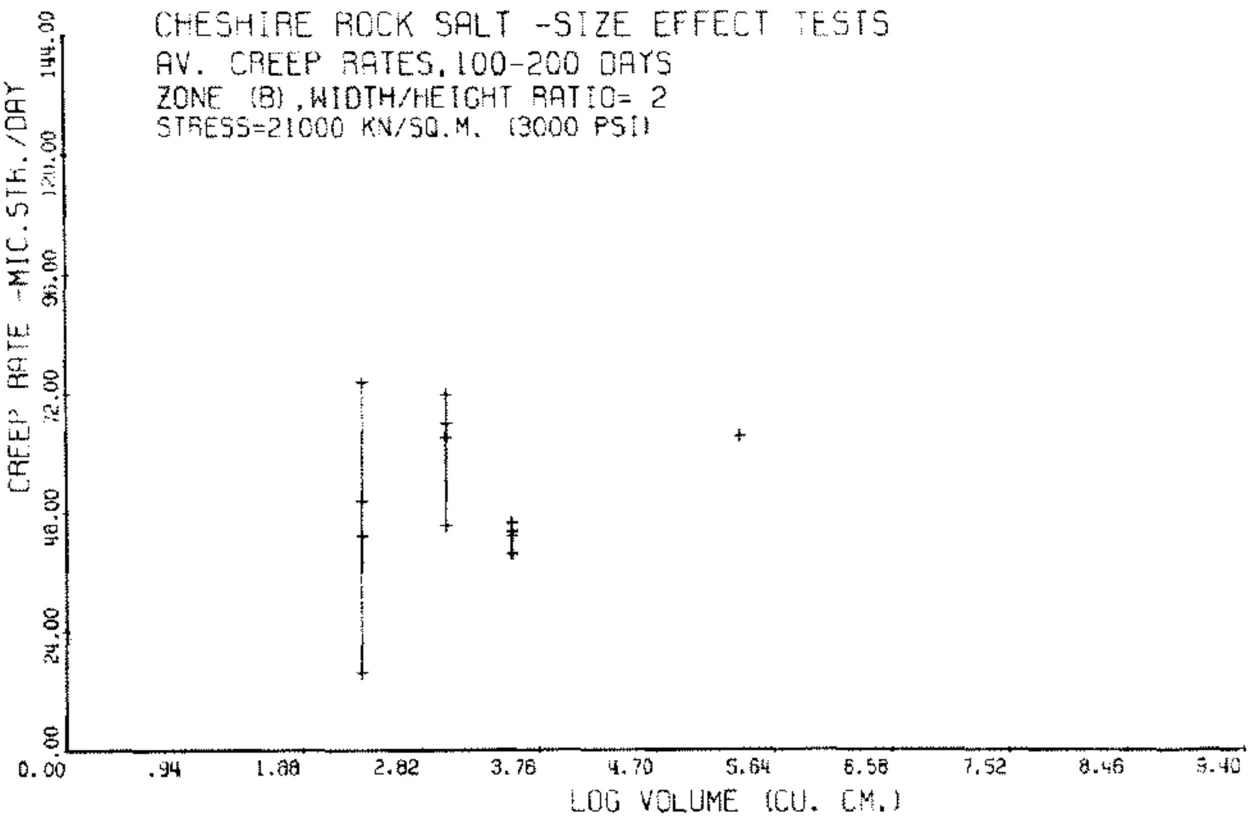

Figure 12. Creep rates for the period from 100 to 200 days as a function of log Volume for Zone B.

any particular volume, but the trend indicates a slightly increasing deformation (or creep) rate with increasing volume, both for Zone B and Zone F salt.

THE DIFFERENTIAL BEHAVIOR OF SPECIMENS FROM ZONES B AND F

Since one of the aims of the research was to investigate the differential behavior of the specimens from Zones B and F, the following Table 4 was extracted from Table 3 and shows the mean creep rates 'B' for the period from 100 to 200 days. When a single test is available, the value of the creep rate is taken to represent the mean. Table 4 demonstrates that Zone B specimens creep faster than those of Zone F for a given volume. However, this differential behavior reduces as the specimen volume increases. These findings are in agreement with the expectation that with large volumes, the effects of the individual behavior of the grains is reduced when the specimen volume becomes adequately large.

TABLE 4

Comparison Between the Differential Behavior of Zone B and Zone F Salt

Volume $\times 10^{-3}m^3$	Zone B $\mu\epsilon$/day	Zone F $\mu\epsilon$/day	Percentage Difference
0.2212	46.00	27.72	39.74
1.0242	61.72	55.34	10.34
3.4566	43.40	39.78	8.34
8.1935	—	68.94	—
22.4831	—	55.21	—
47.7847	—	60.18	—
221.2254	63.68	60.13	5.57

Upon comparing the creep rates of the specimens 30. U and 30. L (Table 3), it is found that, while the differential behavior amounts to 5.57% (Table 4) for the period from 100–200 days, this amount remains almost the same for the next 100 days i.e. over the period from 200 to 300 days. Thus it is suggested that Zone B specimens creep faster than Zone F specimens by at least 5% at any instant of time.

MATHEMATICAL DESCRIPTION OF THE VOLUME EFFECT

In order to utilize the data for extrapolation a function has to be found which provides an acceptable approximation of the expected strain rate as a function of volume. Because more data were available for Zone F salt a logarithmic curve was fitted to the data which is representative of the volume effect. The curve is shown on Fig. 11 as a full line. The equation of the logarithmic curve is:

$$\dot{\epsilon} = \frac{\log_{10} V}{0.0038881 + 0.009392 \log_{10} V} \quad (1)$$

where $\dot{\epsilon}$ = the creep rate in $\mu\epsilon$/day for the period 100 −200 days

and V = Volume in cm^3.

(The volume is expressed as cm^3 for mathematical convenience)

The relationship between volume and strain rate was established for particular conditions, i.e. for a stress level of 21 MN/m^2, a W/H ratio of 2 and for a time period between 100 and 200 days. In order to make use of this relationship for diverging conditions a functional relationship must be established for the conditioning parameters. In general form this can be written as:

$$\dot{\epsilon} = \frac{\log_{10} V}{0.0038881 + 0.009392 \log_{10} V} \cdot f_1(t) \cdot f_2(\sigma) \cdot f_3\left(\frac{W}{H}\right) \quad (2)$$

The effect of stress, and the width to height ratio upon the strain rate as a function of time was investigated by long-term creep tests of model pillars separately (8) (9). The equation for creep rate which was derived from the analysis of model pillar experiments is:

$$\dot{\epsilon} = 1.520 \cdot \sigma^{2.7} \cdot t^{-0.94} \cdot (W/H)^{-0.477} \quad (3)$$

(σ is given in MPa, t in days, and W/H is dimensionless)

Because the volume of the model pillars was less than 0.0021 m^3 hence the above equation cannot be extrapolated to mine pillar sizes without taking the size effect into consideration. By direct comparison of the two equations we may conclude that the unknown functions in equation 2 are those expressed in equation 3, i.e.

$$f_1(t) = t^{-0.94};\ f_2(\sigma) = \sigma^{2.7} \text{ and } f_3(W/H) = (W/H)^{-0.477}$$

and these can be substituted into equation 2.

The constant 1.52 in equation 3 cannot be substituted directly because the equation 2 was derived for particular conditions, t = 150 days, σ = 21.0 MN/m^2 and W/H = 2.

In order to determine the constant to fit the measured data the strain rate for the largest specimen, $0.221 \times 10^{-3} m^3$, and the conditioning parameters were substituted into equation 3. This substitution yielded a new constant and the equation for strain rate can be expressed as:

$$\dot{\epsilon} = 0.0414 \frac{\log_{10} V}{0.0038881 + 0.009392 \log_{10} V} \cdot \sigma^{2.7} \cdot t^{-0.94} \cdot (W/H)^{-0.477} \quad (4)$$

The dimensions of the parameters are the same as before.

The validity of this equation must be checked before it could be used with confidence for extrapolation. For a given underground pillar the volume of the pillar, the time elapsed after pillar isolation and the W/H ratio can be readily determined. The stress determination, however, is a relatively cumbersome process which requires special skills, sophisticated instruments and measuring technique. The stress level in a pillar within a panel was determined by the overcoring technique. The strain changes due to stress relief on the circumference of a 50 mm borehole were monitored continuously during overcoring by the Talbott strain cell, and the calculated strains were converted into stresses by multiplying the strains by a factor corresponding to the in situ Modulus of Elasticity of the rock mass. The strain cell and technique is described by Miller et al. (10).

The pillars in which the in situ stress level was measured had a W/H ratio of 2, was isolated 14 years ago and the measured stress in the pillar was 16.2 MPa. The dimensions of the pillar were 15.24 × 15.24 × 7.62 m = 1.76980×10^9 cm^3. Substituting these values into equation 4:

$$\dot{\epsilon} = 41.4 \times 10^{-3} \frac{\log_{10} 1.76980 \times 10^9}{38.881 \times 10^{-6} + 9.392 \times 10^{-6} \cdot \log_{10} 1.7698 \times 10^9}$$

$$(14.365)^{-0.94} \cdot 16.2^{-2.7} \cdot 2^{-0.477}$$

$$\dot{\epsilon} = 1.32\ \mu\epsilon/\text{day}$$

The strain at the center of the pillar was measured by the optical deformation measurement technique (8) and the strain rate in the fourteenth year of the pillar was found to be $\dot{\epsilon}$ = 1.05 $\mu\epsilon$/day, which compares favorably with the extrapolated value.

CONCLUSIONS

The experimental data and the favorable agreement between the measured and predicted strain rate for a salt pillar confirms the well-grounded presumption that the "volume-effect" is rather small in respect of creep behavior of a fairly homogenous rock salt mass. This is understandable because by nature of the rock salt, cracks or weakness planes are non-existent, or if these existed then these are already "healed" due to creep of the material. The scatter in the results for small size specimens is probably due to the uneven distribution of marl within the sample and the variation of the size of the salt grain.

Another aspect of the experiments indicate that it would be economical to test larger size specimens in the laboratory but less in number to obtain the representative material constants.

REFERENCES

1. Jaeger, J.C. and Cook, N.G.W. 1976. Fundamentals of Rock Mechanics. Chapman and Hall, London, 183−194.

2. Troxell, G.E., Rapheal, J.M. and Davies, R.E. 1958. Long-term Creep and Shrinkage Tests of Plain and Reinforced Concrete. Am. Soc. Testing Materials. Proc. 58: 1102–1112.

3. Guilford, J.P. 1971. Fundamental Statistics in Psychology and Education. Kogakusha Company Ltd., Tokyo, 356–391.

4. Graybill, F.A. 1961. An Introduction to Linear Statistical Models. McGraw-Hill Book Co., New York, 93–105.

5. Durbin, J. and Watson, G.S. 1951. Testing for Serial Correlation in Least Squares Regression–II. Biometrika, 38: 159–178.

6. Draper, N.R. and Smith, N.M. 1967. Applied Regression Analysis. John Wiley and Sons, New York, 86–103.

7. Smillie, K.W. 1966. An Introduction to Regression and Correlation. The Ryerson Press, Toronto, 1–29.

8. Potts, E.L.J., Potts. W.H. and Szeki, A. 1972. Development of Ground Control Techniques and Mining Design Parameters in Rock Salt Mining. 5th Int. Strata Control Conf., London, Paper No. 26.

9. Mirza, U.A.A. 1978. Investigation into the Design Criteria for Underground Openings in Rocks which Exhibit Rheological Behavior. Ph.D. Thesis, University of Newcastle upon Tyne.

10. Miller, H.D.S., Potts, E.L.J., Szeki, A. and Talbott, A.C. 1977. Part I: Development of a Borehole Strain Cell for In-situ Stress Determination in Rock, Part II: In-situ measurements in Halite in Cheshire, Potash in North Yorkshire and Slate at Dinorwic. Conf. on Rock Engineering Proc., University of Newcastle upon Tyne, The British Geotechnical Society, London, 245–256 and 257–274.